



**HAL**  
open science

# Recovery of nisin from culture supernatants of *Lactococcus lactis* by ultrafiltration: flux properties and separation efficiency

Adrien Forestier, Yanath Belguesmia, François Krier, Djamel Drider, Pascal Dhulster, Loubna Firdaous

## ► To cite this version:

Adrien Forestier, Yanath Belguesmia, François Krier, Djamel Drider, Pascal Dhulster, et al.. Recovery of nisin from culture supernatants of *Lactococcus lactis* by ultrafiltration: flux properties and separation efficiency. *Food and Bioproducts Processing*, 2022. hal-04545772

**HAL Id: hal-04545772**

**<https://hal.science/hal-04545772>**

Submitted on 14 Apr 2024

**HAL** is a multi-disciplinary open access archive for the deposit and dissemination of scientific research documents, whether they are published or not. The documents may come from teaching and research institutions in France or abroad, or from public or private research centers.

L'archive ouverte pluridisciplinaire **HAL**, est destinée au dépôt et à la diffusion de documents scientifiques de niveau recherche, publiés ou non, émanant des établissements d'enseignement et de recherche français ou étrangers, des laboratoires publics ou privés.

**Recovery of nisin from culture supernatants of *Lactococcus lactis* by ultrafiltration: flux properties  
and separation efficiency**

Adrien FORESTIER, Yanath BELGUESMIA, François KRIER, Djamel DRIDER, Pascal DHULSTER and  
Loubna FIRDAOUS\*

UMR Transfrontalière BioEcoAgro N° 1158, Univ. Lille, INRAE, Univ. Liège, UPJV, YNCREA, Univ. Artois,  
Univ. Littoral Côte d'Opale, ICV – Institut Charles Viollette, F-59000 Lille, France

\*to whom correspondence should be addressed

[loubna.firdaous@univ-lille.fr](mailto:loubna.firdaous@univ-lille.fr)

## Abstract

Nisin is a class I bacteriocin, which is produced by lactic acid bacteria (LAB) belonging to *Lactococcus* and *Streptococcus* genera. Nisin is approved by the FDA (Food and Drug Administration) as a natural biopreservative agent under reference E234. Besides food application, nisin has also a potential for therapeutic application to treat a range of infectious diseases. Nisin, which is commercially available, is mainly produced by liquid fermentation. The production of commercial high-quality nisin is hampered by the high cost of downstream processing, which often involves subsequent steps of salt precipitation, centrifugation, and chromatography. Membrane processes offer a set of advantages. Indeed, these processes are simple and effective technologies for protein concentration and separation; One of the biggest limitations is the decrease in permeate flux. In this study, the performance of three UF membranes (10, 50, and 100 kDa) for the separation and concentration of nisin obtained from *Lactococcus lactis* (*L. lactis*) culture supernatants was evaluated. Permeate flux decline, fouling resistances, fouling index, nisin recovery in the permeate and retentate streams were evaluated. The 10 kDa membrane showed the best nisin recovery properties with the highest recovery yield and purification factor, achieving 100% and 4 in the retentate stream, respectively.

## Highlights

- Ultrafiltration is a promising process for the recovery and concentration of nisin from complex culture supernatants.
- Three MWCO (10, 50 and 100 kDa) were tested for membrane fouling and nisin recovery from *Lactococcus lactis* culture supernatants.
- All membranes tested caused fouling during ultrafiltration.
- Resistance in series model and Hermia's model were used to investigate fouling mechanisms.
- The 10-kDa membrane enabled the highest recovery of nisin and the highest purification factor, reaching 100% and 4 in the retentate stream, respectively.

**Keywords:** ultrafiltration, downstream processing, nisin, separation, fouling, recovery

## 1. Introduction

Bacteriocins are ribosomally synthesized peptides produced by Gram-positive and Gram-negative bacteria as well as by Archaea [1] and have a broad spectrum of antimicrobial activity at low concentrations [2]. Although the first bacteriocin identified was colicin, produced by *Escherichia coli* in 1925 [3], bacteriocins produced by food grade LAB have been studied most intensively because of their non-toxic nature and high bactericidal activity in the nanomolar range [4].

Nisin is produced by LAB bacteria belonging to *Lactococcus* and *Streptococcus* genera [5]. Nisin also designed as lantibiotic contains noteworthy unusual amino-acids like lanthionine and methyllanthionine. Nisin is a 34 amino- acids, hydrophobic polypeptide with an isoelectric point above 8.5 and a molecular mass of 3,352 Da [6].

Nisin is active against a set of Gram-positive bacteria such as *Staphylococcus aureus*, *Listeria monocytogenes* and *Clostridium* species [7]. This trait, combined with GRAS (generally considered as safe) status contributed to the worldwide success of nisin as a natural food preservative under reference E234 [8]. Nisin has also additional benefits in the medical sector as a potential therapeutic agent for controlling bacterial infections. One of the most promising options is the use of this bacteriocin in the treatment of local and topical infections such as diseases of the oral cavity, skin, respiratory tract, stomach, intestine or mammary gland [9,10].

The worldwide nisin market has reached USD 317.9 million in 2020 and is expected to grow yearly at an average rate of 7.3 % in the period 2021 - 2030 [11]. However, the production cost of nisin is a major bottleneck making it difficult to meet the growing market demand. For its industrial use, nisin is obtained from *L. lactis* subsp. *lactis* and marketed as Nisaplin (Danisco, Denmark), in the form of a dried concentrated powder containing 2.5% nisin with NaCl (77.5%) and denatured milk proteins (12% protein and 6% carbohydrate), and licensed as a food additive E234 in more than 60 countries [12]. Even the industrial isolation and purification methods used are not described in details in the literature, it has been referred that nisin production is carried out in batch fermentation systems with *L. lactis* in supplemented whey or milk medium, and purified by successive steps of foam or filtration concentration, followed by salt precipitation, centrifugation, spray drying and pin milling [13].

As a high value bioproduct, nisin's downstream processing consists of four stages: clarification, separation and concentration, purification and finally polishing. The concentration (as the first step after the primary clarification of culture medium) plays an important role not only for the next purification steps but also for the concentration of these products without significant reduction in biological activity [14]. Several studies have been carried out on the separation and concentration of nisin, particularly ammonium sulfate precipitation, solvent extraction and chromatography, and many authors have reported different yields and purification factors [14,15]. Ammonium sulfate precipitation for the initial concentration of nisin is the most preferred method [16]. Other reported

processes to concentrate nisin include solvent extraction with organic solvents such as toluene [17], chloroform [18], ethanol and methanol [19]. Aqueous two-phase micellar systems using Triton X-100 and X-114 as surfactants have also been proposed [20,21]. Although the selective extraction of nisin has been demonstrated, these processes can introduce compounds that may be of regulatory concern for food applications and their implementation on an industrial scale implementation has therefore been considered challenging.

Pressure-driven membrane processes, such as ultrafiltration (UF) and nanofiltration (NF) are useful tools for fractionation, concentration, recovery and purification of high-added value bioproducts [22] and are already used at industrial scale. High separation efficiency, easy scale-up, simple operation, high productivity, and absence of phase transition are decisive advantages of membrane processes over conventional separation technologies. According to the literature, ultrafiltration and nanofiltration have attracted the attention of bacteriocin's researchers to selectively separate bacteriocins from fermentation broths [23,24]. To the best of our knowledge, however, only a few systematic studies were devoted to the use of pressure-driven membrane processes in the downstream processing of bacteriocins.

This study focuses on the use of ultrafiltration as a pre-purification step in the downstream processing of nisin. In this context, three polymeric membranes with MWCOs of 10, 50, and 100 kDa were tested during the ultrafiltration of *L. lactis* supernatants containing nisin. Membrane selection has been related to the size of the contaminating proteins and also to nisin, which has the property of forming dimers (7,000 Da) and tetramers (14,000 Da) in solution [6]. It has also been reported in the literature that bacteriocins are retained very efficiently by UF membranes with a MWCO of 10 kDa [25]. Therefore, the performances of these membranes in terms of nisin recovery, contaminating proteins removal, permeate flux, membrane fouling and cleaning efficiency have been then evaluated and discussed.

## **2. Materials and methods**

### **2.1. Materials and bacterial strains**

The nisin used as a positive control and standard in this study was a commercial powder from *L. lactis* 2.5% (Sigma Aldrich, St. Louis, Mo, U.S.A.). The nisin-producing strain used was *L. lactis* subsp. *lactis* DSM 20729 (DSMZ, Braunschweig, Germany). The antimicrobial activity of nisin was tested against *Listeria innocua* CIP 80.11 (Institut Pasteur, Lille, France). The strains were stored at -80°C and -20°C in M92 broth (*L. lactis*) and BHI Broth (*L. innocua*). The broths were supplemented with glycerol until 20% (v/v) was reached.

### **2.2. Nisin production by *Lactococcus lactis***

Nisin production was studied in different media at 30°C in static culture: BHI (Sigma Aldrich, St Louis, Mo, USA), M17 (Sigma Aldrich, St Louis, Mo, USA) and citrate milk using *L. lactis* DSM 20729 as a producing strain. Citrate milk medium was chosen as it yielded the highest antimicrobial activity in the supernatant (64 AU. mL<sup>-1</sup>). Citrate milk medium consisted of 8.0 g. L<sup>-1</sup> sodium citrate, 1.0 g. L<sup>-1</sup> yeast extract, 5.0 g. L<sup>-1</sup> glucose and 50.0 g. L<sup>-1</sup> skim milk with a pH between 6.8 and 7.2, and sterilized at 110°C for 10 minutes.

For each nisin production, *L. lactis* DSM 20729 was activated from frozen storage (-20°C) by incubation in citrate milk medium for 24h at 30°C in static state. The *L. lactis* strain was subcultured twice at 1% (v/v) under the same conditions. *L. lactis* DSM 20729 was incubated at 1% (v/v) directly in two sterile centrifugation tubes with 350 mL of medium in each tube under the same conditions. After centrifugation for 20 minutes at 4800 g, the acidic supernatant was kept at 4°C for less than 24 hours before ultrafiltration experiments.

### 2.3. Assessment of antimicrobial activity

*L. innocua*, selected for its sensitivity to nisin, was revived from frozen storage (-20°C) by incubation in BHI broth at 37°C without shaking for 24h and subcultured twice under the same conditions before being used for the antimicrobial activity assay. Antimicrobial activity was determined by a microcritical dilution method using a microtiter plate. The samples were neutralized to pH comprised between 6 and 6.5 by adding NaOH 2.5 M and then sterile-filtered (PES filter 0,2 µm). Serial two-fold dilutions of sterile samples were prepared in 125 µL volumes of sterile BHI broth in a sterile Costar 96-well flat-bottom microtiter plate (Corning Incorporated, Kennebunk, USA). Each well was then inoculated with 50 µL of *L. innocua* culture. The plates were then incubated without shaking at 37°C for 18 hours to 24 hours before absorbance measurement was performed at 630 nm with an ELx808tm microplate reader (BioTek Instruments Inc, Winooski, Vermont, USA). An arbitrary unit (AU) was defined according to [26]:

$$AU = \frac{1}{V} \times D \quad (1)$$

where V is the sample volume in mL and D is the highest dilution factor at which growth is inhibited.

### 2.4. Ultrafiltration experiments

#### 2.4.1. Membranes and filtration system

Ultrafiltration experiments were carried out on a laboratory-scale using LABCELL CF-1 membrane filtration unit (Koch Membrane Systems, Stafford, United Kingdom). The system consists of a flat cell of 75 mm with a membrane effective area of 28 cm<sup>2</sup>, a double wall feed tank with 500 mL process volume, a pressure gauge (1 – 10 bar), a pressure control valve and a feed/recirculation pump (Figure 1). In order to keep the temperature of the feed solutions constant, the tank double wall was fed with

tap water. A thermometer located in the feed tank was used to monitor the temperature of the feed solution during the process. The transmembrane pressure (TMP) was controlled by the valve on the retentate side.

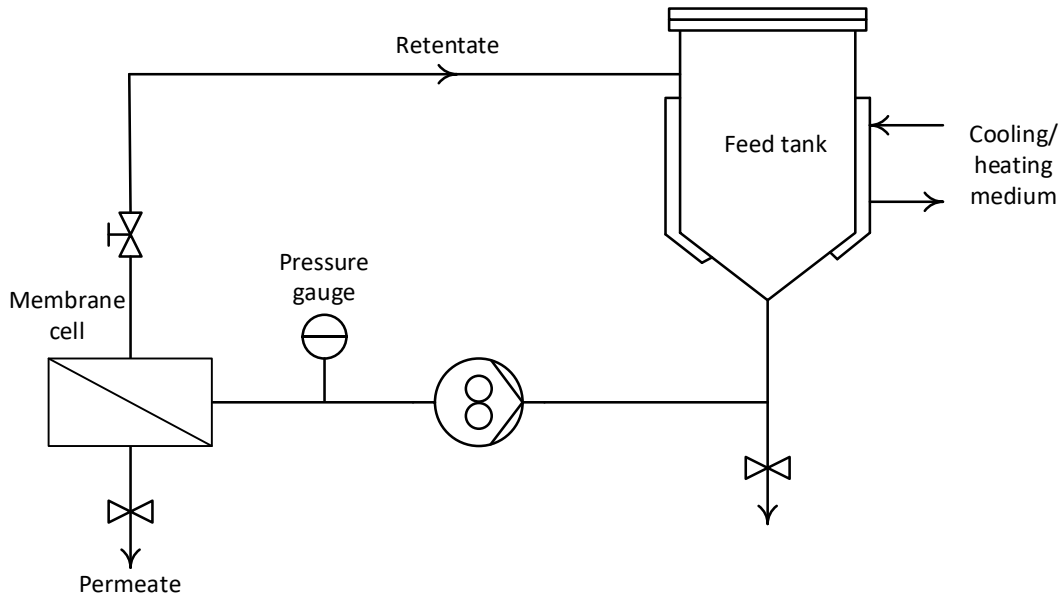


**Figure 1: Schematic experimental setup for ultrafiltration process**

HyStream TangenX flat sheet membranes from REPLIGEN (Waltham, Massachusetts, USA) with MWCOs 10, 50, and 100 kDa were used for experiments. They were selected for their excellent performance, high permeate flux, and low protein adsorption, as recommended in the literature [27]. Information and properties of the selected membranes are listed in Table 1.

**Table 1: Properties of selected Hystream TangenX membranes from the manufacturer**

Item	Description
<b>Substrate composition - Thickness</b>	Non-woven polypropylene - 160 Microns
<b>Membrane composition - Thickness</b>	Modified PES - 70 microns
<b>Hydrophilicity (contact angle)</b>	4 degrees (high hydrophilic properties)
<b>Membrane charge</b>	Neutral
<b>Effective filtration area</b>	28 cm <sup>2</sup>
<b>Maximum running pressure</b>	7 bar
<b>pH range</b>	1 – 14

Before the ultrafiltration experiments, all the membranes were subjected to a measurement of the pure water flux ( $J_{w0}$ ) at different transmembrane pressures. The pure water permeability  $L_{p0}$  of each membrane was obtained from the slope of the calibration curve to an axis intercept equal to zero, according to:

$$J_{w0} = L_{p0} \times \Delta P = \frac{\Delta P}{\mu R_m} \quad (2)$$

where  $J_{w0}$  is the water permeation flux ( $\text{m}^3 \cdot \text{m}^{-2} \cdot \text{s}^{-1}$ ),  $L_{p0}$  is the pure water permeability ( $\text{m} \cdot \text{s}^{-1} \cdot \text{Pa}^{-1}$ ),  $\mu$  is the water viscosity ( $\text{Pa} \cdot \text{s}$ ), and  $R_m$  is the intrinsic membrane resistance ( $\text{m}^{-1}$ ).

#### 2.4.2. Ultrafiltration protocol

Culture supernatants from *L. lactis* DSM 20729 were used for ultrafiltration experiments. For the selection of the transmembrane pressure for the concentration mode, the first experiments were performed in total recirculation mode at different TMPs. Both retentate and permeate streams were recirculated into the feed tank to maintain a constant feed concentration. The runs were performed in the transmembrane pressure range of 0.75 - 5 bar. Temperature and cross flow velocity were kept constant at 20°C and 1.7  $\text{m} \cdot \text{s}^{-1}$ , respectively. Each transmembrane pressure level was maintained for 10 min until the permeate flux had stabilized.

Concentration experiments were performed in batch mode, with simultaneous retentate recycle and permeate removal. The experiments were carried out at a constant transmembrane pressure of 2 bar (selected pressure). The ultrafiltration was operated up to a volume reduction factor of 5 (VRF, defined as the ratio between the initial feed volume and the volume of the resulting retentate). The permeate flux was continuously monitored during the experiments and samples were taken from both the retentate and the permeate at volume reduction factor (VRF) 1.5, 2, 3 and 5.

The experiments were run with an initial volume of 500 mL, a cross-flow velocity of 1.7  $\text{m} \cdot \text{s}^{-1}$  and a constant temperature of 20°C. The pH and conductivity of all samples taken during each experiment were determined. The samples were stored at 4°C for analysis.

At the end of the filtration, the laboratory-scale **pilot** was empty and the following cleaning procedure was performed to recover the initial membrane permeability. First, the membrane was rinsed with distilled water for 10 minutes in order to drag the reversible foulants. During the rinsing step, a TMP of 2 bar and a temperature of 20°C were applied and the retentate was discarded in order to prevent the deposition of the foulants on the membrane surface. At the end of rinsing, the pure membrane water permeability was measured ( $L_{p1}$ ). The membranes were then subjected to a chemical cleaning to restore the initial permeate fluxes. The chemical cleaning step was carried out at a TMP of 2 bar and a temperature of 40°C, and by recirculating 500 mL aqueous NaOH 0.02 M with 3mL of 3.6% aqueous NaClO for 90 min. A final rinsing step was performed by recirculating 500 mL of distilled water at 20°C until a neutral pH was reached.

At the end of the cleaning procedure, the pure water permeability was measured again ( $L_{p2}$ ) and the cleaning efficiency (CE) was evaluated according to [28]:

$$CE = \left( \frac{L_{p2}}{L_{p0}} \right) \times 100 \quad (3)$$



where  $L_{p2}$  is the water permeability after cleaning ( $\text{m. Pa}^{-1} \cdot \text{s}^{-1}$ ) and  $L_{p0}$  is the water permeability of the new membrane ( $\text{m. Pa}^{-1} \cdot \text{s}^{-1}$ ). The fouling index (FI) was also assessed by comparing the water permeation flux before and after the ultrafiltration [29]:

$$FI = \left(1 - \frac{L_{p1}}{L_{p0}}\right) \times 100 \quad (4)$$

where  $L_{p1}$  is the water permeation flux after ultrafiltration ( $\text{m. Pa}^{-1} \cdot \text{s}^{-1}$ ).

All experiments were performed in triplicate and the results expressed as means and standard deviations. A new membrane was used for each replicate.

## 2.5. Analytical methods

Culture supernatant, permeate and retentate samples from various experiments were stored for less than 3 days at 4°C for analysis. The samples were analyzed in terms of dry matter, ash and total protein content, antimicrobial activity, and molecular weight distribution (SDS-PAGE).

### 2.5.1. Dry matter and ash contents

The dry matter content in the samples was measured by drying at 105°C using a Precisa XM60 infrared moisture analyzer (Precisa Gravimetrics AG, Dietikon, Switzerland). Ash content was estimated by drying the samples in a ceramic crucible at 105°C for 3 hours before placing them in a muffle furnace at 550°C overnight. The ceramic crucible was cooled in a desiccator at room temperature for 30 minutes before being weighed. The ash content (% dry basis) was estimated as follows: (mass of ash/mass of the dry matter contained in the initial sample)  $\times$  100. Each analysis was performed in triplicate.

### 2.5.2. Protein concentration measurement

The protein content of each sample was determined using the BCA protein assay reagent (Sigma Aldrich, St. Louis, MO, USA). The tests were performed on glass hemolysis tubes by mixing 0.1 mL of the sample with 2 mL of the reagent for 30 minutes at 37 °C. The tubes were then cooled to room temperature for 15 minutes and the absorbance was read at 562 nm on a Secomam UV-visible Prim Advanced spectrophotometer (Secomam, Dormont, France). The concentration was calculated (in  $\text{mg. mL}^{-1}$ ) using a calibration curve based on BSA with a concentration range of 0.2 – 1  $\text{mg. mL}^{-1}$  ( $R^2 = 0.9954$ ). Samples with an absorbance reading greater than 1 were diluted and retested. Each assay was run in triplicate.

### 2.5.3. Sodium dodecyl sulfate–polyacrylamide gel electrophoresis (SDS–PAGE)

SDS-PAGE analysis was performed to qualitatively assess the composition of the permeates and retentates obtained from UF experiments. Briefly, samples were combined with an equal volume of sample buffer Novex Tricine SDS Sample Buffer (2X) (Invitrogen, Carlsbad, USA) and were heated to 90°C for 5 minutes (denaturation under reducing conditions). The samples were then applied in Mini-

Protean® Tris-Tricine 16.5% ready-made gels (BioRad Laboratories, Hercules, CA, USA). The loading volume for each sample was 20 µL. Two polypeptide protein molecular weight markers (10 kDa – 250 kDa and 1.4 kDa – 26.6 kDa) (BioRad Laboratories, Hercules, CA, USA) were used for calibration. Electrophoresis was performed at a constant voltage of 100 V for 80 minutes using a Mini-Protean II system (BioRad Laboratories, Hercules, CA, USA). The gels were stained with InstantBlue™ (Expedeon, Cambridgeshire, UK) overnight and then rinsed with distilled water until the background color disappeared. The SDS-PAGE gels were then scanned using a Geldoc calibrated densitometer from Bio-Rad (Hercules, CA, USA).

## 2.6. ATR-FTIR spectroscopy measurements

To characterize membrane fouling, ATR-FTIR measurements were performed using a Thermo Nicolet iS50 FTIR (Thermo Fisher Scientific, Waltham, MA, USA) spectrometer equipped with a single-bounce diamond crystal and a deuterated triglycine sulfate (DTGS) detector. XT-KBr was utilized as the beamsplitter.

For each MWCO tested, ATR-FTIR measurements were carried out for both virgin and fouled membranes. Before analysis, the membranes were dried at 60°C for at least 24 h to remove any water residue. The spectra were scanned between 4000 and 400 cm<sup>-1</sup> in attenuated total reflectance (ATR) mode. A total of 64 scans were averaged for each sample at a 4 cm<sup>-1</sup> resolution, and subsequently, the IR spectra were processed using the OMNIC software (Nicolet, Madison, USA). The recorded spectra were treated by subtracting the virgin membrane spectrum from that of the fouled membrane leaving only the ATR spectrum of the foulants.

## 2.7. Data processing

The permeate flux ( $J_p$ ) was determined by measuring the collected volume of permeate in a given time through the membrane surface area as:

$$J_p = \frac{V_p}{A \times t} \quad (5)$$

where  $J_p$  is the permeate flux (m<sup>3</sup>.m<sup>-2</sup>.s<sup>-1</sup>),  $V_p$  is the permeate volume (m<sup>3</sup>) at time  $t$  (s) and  $A$  is the membrane surface area (m<sup>2</sup>).

A percentage of the mass balance (MB) for dry matter, ash and protein was calculated according to:

$$MB(\%) = \frac{C_p V_p + C_r V_r}{C_0 V_0} \quad (6)$$

Where  $C_p$ ,  $C_r$  and  $C_0$  are each either the dry matter, ash or the protein concentration in the permeate, in the retentate and in the supernatant,  $V_p$ ,  $V_r$  and  $V_0$  are the respective volumes in each case.

The ultrafiltration effectiveness for the selective separation of nisin has been described in terms of the yield of the antimicrobial activity ( $Y_A$ ), the activity balance (AB%) and purification factor ( $P_F$ ). These parameters were calculated using the following equations:

$$Y_A = \frac{A_F \times V_F}{A_0 \times V_0} \times 100 \quad (7)$$

where  $A_F$  and  $A_0$  are the total antimicrobial activity in the final recovery solution and the initial solution, respectively.  $V_F$  and  $V_0$  are the respective volumes in each case.

$$AB\% = \frac{A_P V_P + A_R V_R}{A_0 V_0} \quad (8)$$

where  $A_P$ ,  $A_R$  and  $A_0$  are the total antimicrobial activity in permeate, retentate and initial culture supernatant, respectively.  $V_P$ ,  $V_R$  and  $V_0$  are each the respective volumes.

The purification factor,  $P_F$ , determined as the ratio of the specific antimicrobial activity in the final solution and the original specific antimicrobial activity in the starting solution, was calculated as follows:

$$P_F = \frac{SA \text{ in final solution}}{SA \text{ in initial solution}} \quad (9)$$

where SA is the specific activity, which means the activity per amount (mg) of proteins.

## 2.8. Resistance analysis

The resistance-in-series model was applied to quantify membrane fouling. According to this model, flux decline can be described by the total filtration resistance ( $R_t$ ) including membrane hydraulic resistance ( $R_m$ ) and fouling resistance ( $R_{fc}$ ) which can be split into reversible ( $R_{rev}$ ) and irreversible ( $R_{irr}$ ) resistances.

$$J_p = \frac{\Delta P}{\mu R_t} = \frac{\Delta P}{\mu(R_m + R_{fc})} = \frac{\Delta P}{\mu(R_m + R_{irr} + R_{rev})} \quad (10)$$

where  $J_p$  is the permeate flux ( $\text{m}^3 \cdot \text{m}^{-2} \cdot \text{s}^{-1}$ ),  $\Delta P$  is the transmembrane pressure (Pa) and  $\mu$  the permeate viscosity (Pa.s). All resistances ( $R_t$ ,  $R_{fc}$ ,  $R_{irr}$  and  $R_{rev}$ ) are in  $\text{m}^{-1}$ .

$R_m$  was derived from the flux of distilled water,  $J_w$ , according to Eq. (2).  $R_t$  was determined from the steady-state permeate flux,  $J_s$ .  $R_{irr}$  was obtained from the water permeability measurements after the rinsing step. Finally,  $R_{rev}$  was determined by the difference between  $R_t$  and the sum of  $R_m$  and  $R_{irr}$ .

## 2.9. Hermia's model

Besides the quantification of membrane fouling by resistance-in-series model, the fouling mechanisms were estimated by Hermia model.

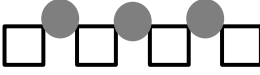
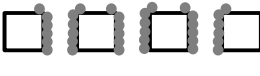
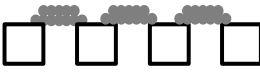
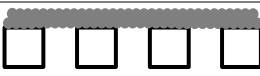
Hermia [30] developed semi-empirical mathematical models based on the classic constant filtration process to describe permeate flux decline.

$$\frac{d^2 t}{dV^2} = k \left( \frac{dt}{dV} \right)^n \quad (11)$$

In this model,  $n$  characterizes the type of filtration mechanism as the complete blocking model, intermediate blocking model, standard blocking model and cake layer model.

The model equations for fouling mechanisms are provided in Table 2.

**Table 2: Membrane fouling mechanisms and models proposed by Hermia**

n value	Fouling mechanism	Illustration	Linear equation
2	Complete pore blocking		$\ln J = \ln J_0 - k_c t$
1.5	Standard pore blocking		$\frac{1}{J^{0.5}} = \frac{1}{J_0^{0.5}} - k_p t$
1	Intermediate pore blocking		$\frac{1}{J} = \frac{1}{J_0} - k_i t$
0	Cake formation		$\frac{1}{J^2} = \frac{1}{J_0^2} - k_t t$

### 3. Results and discussion

#### 3.1. Initial characterization of culture supernatant

According to the literature, the major non-nisin components of *L. lactis* (DSM 20729) culture supernatants, other than water, consist of proteins, peptides, and low molecular weight impurities such as salts, sugars, organic acids and amino acids [31,32]. Because differences in feed composition affect the performance of a membrane process, culture supernatants were characterized in order to plan the membrane fractionations accordingly. The basic properties of the culture supernatants can be seen in Table 3.

**Table 3: Composition and properties of *L. lactis* (DSM 20729) culture supernatants**

Analysis	Mean value	SD
pH	4.70	0.10
Conductivity ( $\mu\text{S. cm}^{-1}$ )	7158	1118
Dry matter (%)	4.16	0.39
Protein ( $\text{g. L}^{-1}$ )	2.35	0.35
Ash (%)	0.74	0.05

An initial SDS-PAGE analysis of *L. lactis* DSM 20729 culture supernatant was also performed to characterize the sizes of the proteins. The results are shown in Figure 2. It displays predominant bands in the 12- 40 kDa range, which can be attributed to the major milk proteins including  $\alpha$ -,  $\beta$ -,  $\kappa$ - casein,  $\beta$ -Lg and  $\alpha$ -La. The remaining bands in the high molecular weight region could correspond to soluble chemical complexes between  $\kappa$ - casein,  $\beta$ -Lg and  $\alpha$ -La [33–35]. A band of about 3,35 kDa in lane 3 is readily visible, advocating the presence of nisin in the culture supernatant [6].

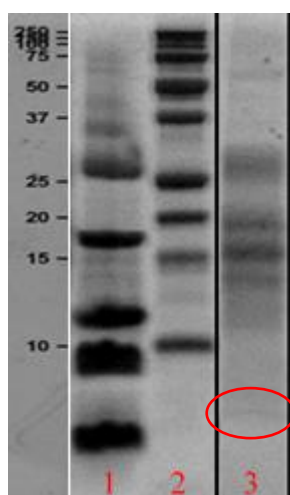


**Figure 2: Sodium dodecyl sulphate polyacrylamide gel electrophoresis (SDS-PAGE) profile of supernatant. Lanes: 1: molecular weight marker from 1.4 to 26.6 kDa, 2: molecular weight markers from 10 to 250 kDa, 3: initial supernatant of *L. lactis* (DSM 20729).**

Based on this initial characterization and literature data, a rough classification of components of *L. lactis* DSM 20729 culture supernatant according to their molar weights is shown in Table 4.

**Table 4: Components and molar weights (in Da) classified in culture supernatant of *L. lactis* DSM 20729**

Macromolecules	Mid-molecules	Small molecules
Whey proteins (14.2 – 66.4 kDa)	Nisin A (3352 Da)	Aminoacids (120 Da)
Casein micelles (~110 nm)	Peptides (variable sizes)	Minerals (30 – 100 Da)
		Organic acids (30 – 500 Da)

---

Nisin multimers (dimers 7000 Da, tetramers 14000 Da)    Sugars (150 – 350 Da)

---

Table 4 clearly shows the complex nature of the culture supernatants. The selected MWCOs (10, 50 and 100 kDa) should allow to observe different selectivity phenomena regarding the retention of macromolecules, nisin and its multimers.

### 3.2. Flux behavior

#### 3.2.1. Water membrane permeability

Prior to membrane fractionation of the culture supernatants to selectively separate the nisin produced, selected membranes were tested for water permeability using distilled water in order to determine the intrinsic membrane resistance and the recovery of the initial flux after cleaning.

The results of the variation of the water permeate flux are shown in Figure 3. Since no fouling occurred, the water flux increased linearly with the transmembrane pressure within the tested range (1-5 bar), depending solely on the membrane resistance [36]. In addition, the results show that the water flux through the membranes increases as the molecular weight cut-off increases. The values were 322, 1061 and 1161 L. h<sup>-1</sup>. m<sup>-2</sup>, respectively, for 10, 50 and 100 kDa membranes at a working TMP of 2 bar (used during the UF of the culture supernatants). This result partly agrees qualitatively with the Hagen-Poiseuille equation. According to this theory, with the same membrane pore structure and pore size distribution, the permeate flux through membranes with larger pores increases. Slight changes in the membrane pore structure with increasing average pore size can explain the lower increase in water permeability between 50 kDa and 100 kDa membranes [37,38].

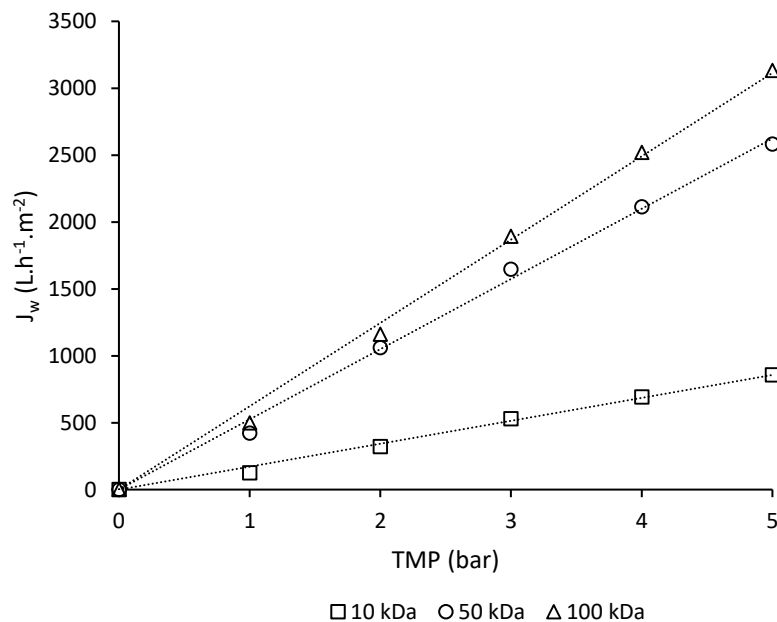


**Figure 3: Water permeate fluxes through the tested ultrafiltration membranes for different TMP at 20 °C**

In the following, the water membrane permeabilities are used as a guide to see to what extent the membranes can be cleaned as described in the membrane cleaning section.

### 3.2.2. Permeate flux in total recirculation mode

According to Section 2.4.2, the recirculation mode was used to investigate the effect of TMP on permeate flux of each membrane tested during the ultrafiltration of *L. lactis* culture supernatants. The TMP was set at different levels from 0.75 to 5 bar and the stable flux value was recorded at each TMP. The permeate fluxes for different TMPs are shown in Fig. 4. The permeate flux increased in a linear relationship with increasing TMP up to approximately 3 bar for 10 and 50 kDa membranes and 2.75 bar for 100 kDa membrane. Then the permeate flux increased slightly and remained almost stable at higher pressures.

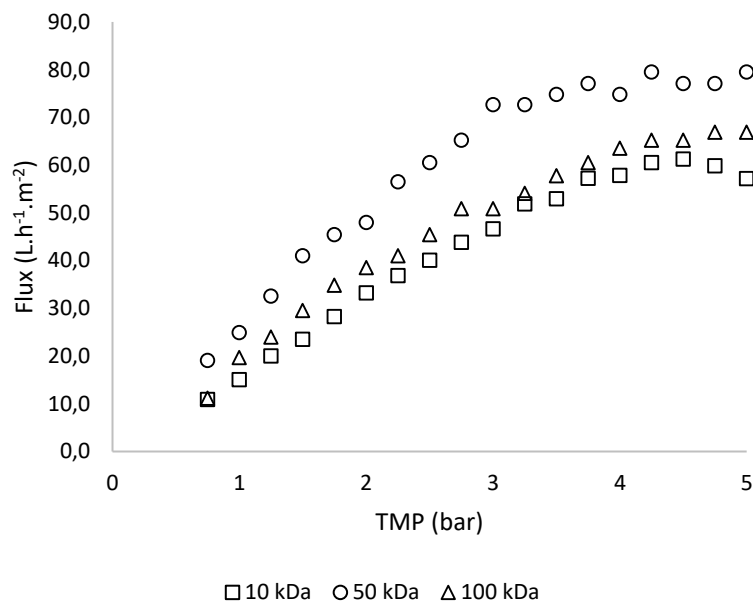


**Figure 4: Variation of permeate fluxes with transmembrane pressure during ultrafiltration of *L. lactis* DSM 20729 culture supernatants. Operating conditions: T = 20°C, v = 1.7 m.s<sup>-1</sup>.**

The permeate flux-TMP curves allowed us to determine the transmembrane working pressure ( $P_w$ ) for ultrafiltration of *L. lactis* culture supernatants with different MWCOs. In fact, the critical transmembrane pressure ( $P_{crit}$ ) represents the TMP at which the permeate flux-transmembrane pressure curve starts to deviate from linearity. In this study, the working TMP ( $P_w$ ) was set at 80% of the critical transmembrane pressure. The results presented in Fig. 4 suggest that a TMP of 2 bar can be regarded as an optimum for the three MWCOs.

### 3.2.3. Permeate flux in concentration mode

For the three membranes tested, the ultrafiltration was carried out in concentration mode until a VRF of 5 was reached. Figures 5a and 5b show the variation of permeate flux during ultrafiltration. Fig. 5a gives the variation with operating time, while Fig. 5b shows the flux-VRF profiles. In all ultrafiltration runs, the permeate flux gradually decreased with the operating time by increasing the volume reduction factor. This drop in permeate flux is typical of membrane filtration and is attributed to a combination of concentration polarization, cake layer formation, solute adsorption and pore clogging as a result of the presence of various components in *L. lactis* DSM 20729 supernatants [39]. This finding confirms what several authors have already observed with the ultrafiltration of milk protein feeds [40,41]. According to Bacchin et al [42], the more concentrated the feed solution is, the lower the permeate flux is. This is due to the higher osmotic pressure and the greater accumulation of solute molecules in the polarization layer, which increases its thickness and consequently its resistance to permeation. The results also show that permeate flux for the 100 kDa membrane is significantly higher than for 50 kDa and 10 kDa membranes. As a result, the time taken to complete the concentration is much shorter. Of the three membranes, 100 kDa showed the higher filtration efficiency: only 79 min to reach VRF = 5 while it was 150 and 356 min for 50 and 10 kDa, respectively.



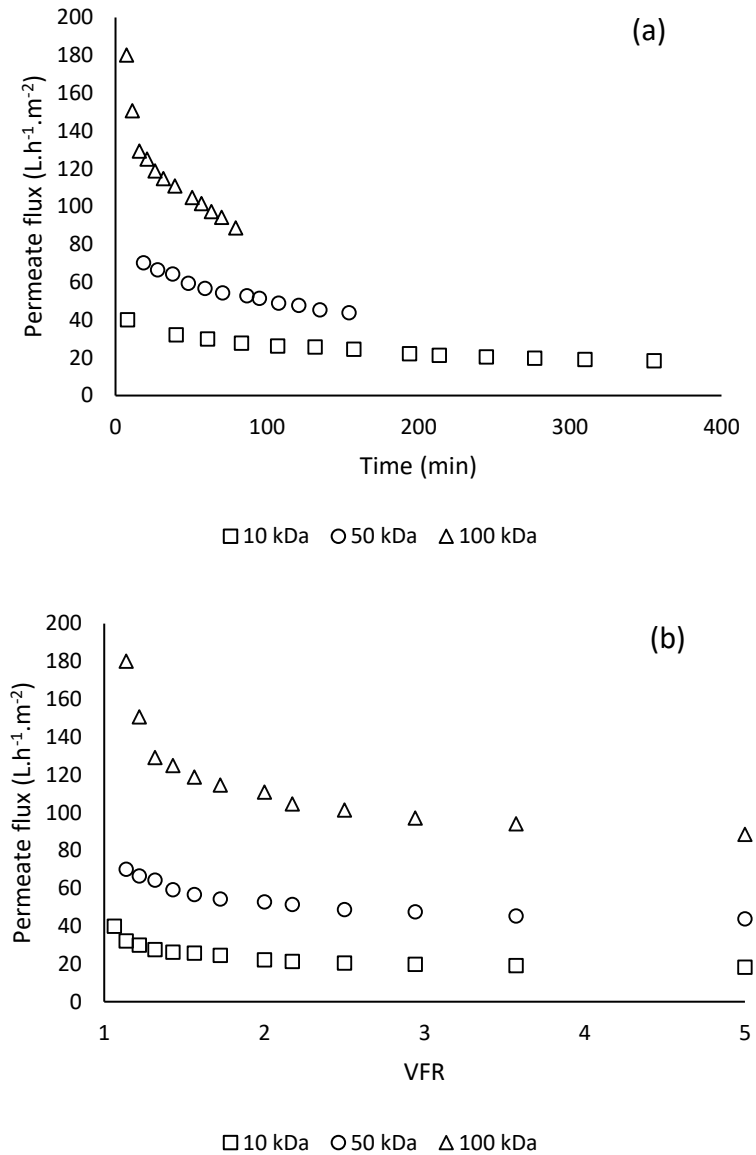


**Figure 5: Mean permeate flux (duplicate) through the tested membranes during ultrafiltration of *L. lactis* DSM 20729 culture supernatants (a) over time and (b) vs. VFR. Operating conditions:  $\Delta P = 2$  bar,  $T = 20^\circ\text{C}$ ,  $v = 1.7 \text{ m}\cdot\text{s}^{-1}$ .**

All permeate fluxes versus VFR profiles (Fig. 5a) could be divided into two stages. The initial stage up to VFR 2 was characterized by a significant flux decline. For 10 kDa and 100 kDa membranes, rapid decrease of approximately 49% and 44%, respectively, in the initial permeate flux were observed. In the case of 50 kDa membrane, the permeate flux decreased by a ratio of 30% over this period. This rapid reduction is attributed to both the adsorption and the irreversible blockage of the membrane pores [43]. The permeate flux was then decreased over time during the increase of VFR from 2 to 5. A decrease in permeate flux of 10% was observed for 10 kDa and 50 kDa membranes and 13% for 100 kDa membrane. During this ultrafiltration stage, in which a quasi-steady state was reached, the combined effects of cake layer formation on the membrane surface and fouling effects should be

significant [44]. The first stage is mainly controlled by foulant–clean membrane interactions (electrostatic, hydrophobic), so its flux depends largely on the membrane properties such as pore size and materials, while the second stage occurs over time under the effect of transmembrane pressure and is independent of the membrane properties (foulant–deposited foulant interaction).

At the end of the ultrafiltration, the mean permeate flux ( $J_p$ ) of the culture supernatants was 19, 44 and 90 L. h<sup>-1</sup>. m<sup>-2</sup> for 10, 50 and 100 kDa membranes, corresponding to 6, 4, and 8% of the membrane water flux, respectively. Chen et al [45] reported similar observations in their experiments and indicate that in biotechnological processes the permeate steady-state flux can be reduced by up to 2% of the water flux determined for the pure membrane.

### **3.3. Membrane fouling analysis**

#### **3.3.1. Fouling index**

The fouling index based on the water permeability before and after ultrafiltration of *L. lactis* (DSM 20729) supernatants was determined for all membranes tested (Table 5). The highest fouling index was measured for 10 and 50 kDa, which had a similar fouling index (90 and 91%, respectively), followed by 100 kDa (82%). These results show that the ultrafiltration process was affected by the membrane fouling phenomenon. The results also indicated that the 10 and 50 kDa membranes fouled more than 100 kDa membrane, confirming the results of the flux decline. These results do not agree with published data that conclude that membranes with large pore sizes are more susceptible to fouling due to pore blocking [46].

In addition, the cleaning efficiency was expressed by permeability recovery after water rinsing and chemical cleaning. Permeability was fully recovered for the 100 kDa membrane, while the fouling was not completely removed for 10 and 50 kDa membranes, for which the cleaning efficiency was 83 and 68%, respectively. This result could be due to irreversible adsorption fouling on the membrane and in the pores.

**Table 5. Water permeabilities, fouling index and productivity of membranes tested in the ultrafiltration of *L. lactis* DSM 20729 supernatants.**

	Membrane MWCO		
	10 kDa	50 kDa	100 kDa
$L_{p0}$ ( $\times 10^{10}$ m. s <sup>-1</sup> . Pa <sup>-1</sup> )	4.51±1.51	15.09±1.03	16.55±1.05
$L_{p1}$ ( $\times 10^{10}$ m. s <sup>-1</sup> . Pa <sup>-1</sup> )	0.59±0.14	1.54±0.27	3.01±0.17
$L_{p2}$ ( $\times 10^{10}$ m. s <sup>-1</sup> . Pa <sup>-1</sup> )	4.00±0.70	10.45±1.94	16.90±2.70
FI (%)	86.96±5.90	89.88±1.68	81.78±0.09
CE (%)	82.97±18.85	67.91±10.66	99.99±9.85
$J_{w0}$ (L.h <sup>-1</sup> .m <sup>-2</sup> )	322.51	1061.64	1160.87
$J_s$ (L.h <sup>-1</sup> .m <sup>-2</sup> )	19	44	90

### 3.3.2. Resistance-in-series-model

In order to further assess the fouling mechanism of the membranes, the different resistances that contribute to flux decline according to the resistance-in-series model (Eq. (11)) were determined. The fouling resistances and the normalized resistances, which show the percentage contribution of each type of resistance to the total, are listed in Table 6.

**Table 6. Resistances during UF of *L. lactis* DSM 20729 supernatants for the tested membranes**

MWCO (kDa)	$R_t$ ( $\times 10^{12}$ m <sup>-1</sup> )	$R_m$ ( $\times 10^{12}$ m <sup>-1</sup> )	$R_{fc}$ ( $\times 10^{12}$ m <sup>-1</sup> )	$R_{rev}$ ( $\times 10^{12}$ m <sup>-1</sup> )	$R_{irr}$ ( $\times 10^{12}$ m <sup>-1</sup> )	$R_m/R_t$ (%)	$R_{fc}/R_t$ (%)	$R_{rev}/R_t$ (%)	$R_{irr}/R_t$ (%)
10	42.29	1.79	40.49	23.20	17.29	4.30	95.70	55.46	40.25
50	15.70	0.63	15.07	8.59	6.48	4.02	95.98	54.69	41.29
100	7.79	0.58	7.22	4.61	2.60	7.41	92.59	59.18	33.41

First, it is important to comment on the calculated values for the  $R_{fc}/R_t$  ratio. According to Aouni et al [47], the fouling phenomenon is considered to be important when the ratio  $R_{fc}/R_t$  is higher than 50%. Considering the values in Table 6, it can be seen that the normalized  $R_{fc}$  was in the range between 92 and 96% for all membranes tested. Therefore, the fouling phenomenon in the ultrafiltration of *L. lactis* DSM 20729 supernatants can be considered significant.

On the other hand, the results obtained clearly show that the total resistance increased with decreasing MWCO. In fact, the highest  $R_t$  value was reported for the 10 kDa membrane. It was 2.7 and 5.4 times more fouled than 50 kDa and 100 kDa membranes in relation to the total filtration resistance. This tendency is expected because a decrease in the MWCO corresponds to a decrease in the pore size of the membrane, which implies a high retention of solutes of a smaller size on the membrane surface [48]. This result also agrees with the sharp decrease in the permeate flux obtained during ultrafiltration of *L. lactis* DSM 20729 supernatants, since an increase in the total resistance means a more hindered passage of the solvent through the membrane, which leads to a decrease in the permeate flux.

Furthermore,  $R_{fc}$  can be divided into a reversible resistance,  $R_{rev}$ , caused by concentration polarization and solute deposition, and an irreversible resistance,  $R_{irr}$ , due to solutes adsorption and pore blocking [49]. Table 6 reveals that overall, the phenomenon of reversible fouling was dominant, since the normalized values of  $R_{rev}$  were higher than those of  $R_{irr}$ . This indicates that the retention of solutes by the membranes occurs mainly on the membrane surface rather than inside the pores and could be explained by a hydrophobic effect. Indeed, milk proteins are known to be hydrophobic, and modified PES membranes used in the current study are highly hydrophilic, according to the membrane manufacturer, and could therefore to some extent prevent the protein molecules from adhering to the membrane surface [50,51]. This also seems to indicate that the present process is quite promising as the flux can be enhanced by improving the hydrodynamic conditions near the surface of the membrane.

To provide a better understanding of the percentage contribution of  $R_{rev}$  and  $R_{irr}$  to the total fouling resistance  $R_{fc}$ , the calculated values of the ratios  $R_{rev}/R_{fc}$  and  $R_{irr}/R_{fc}$  are given in Fig 6.

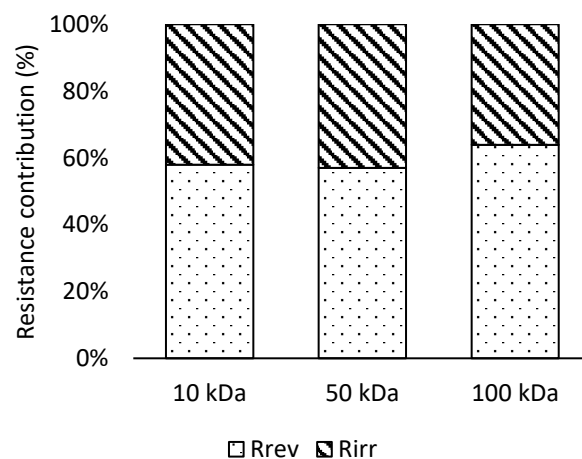


**Figure 6: Contribution of  $R_{rev}$  and  $R_{irr}$  to the total fouling resistance ( $R_{fc}$ ) for the different tested membranes.**

The reversible fouling of the 10 kDa membrane was comparable to that of the 50 kDa membrane; however, the fouling reversibility was more dominant for the 100 kDa membrane. This result suggests that the contribution of reversible fouling resistance increased with increasing membrane permeability. Similar results were reported in other studies in which the reversibility of fouling gradually increased with increasing MWCO of the membrane [52,53]. According to Peeva et al [54], this phenomenon can be explained by the fact that loose membranes were better backwashed due to a higher flow rate, because their resistance was lower than that of the tight membranes. This explanation may support the results of the current study. The 10 kDa and 50 kDa membranes, which exhibited greater membrane resistance, were backwashed less effectively than the 100 kDa membrane at the same pressure.

### 3.3.3. ATR-FTIR analysis

ATR-FTIR analyzes were performed on all the membranes after ultrafiltration experiments and the rinsing step to obtain qualitative information about the foulants responsible for the irreversible fouling. The FTIR spectra for the fouled membranes were obtained and subtracted from the spectrum of the virgin membranes to obtain the spectra of foulants only. The results are shown in Fig. 7.

Several main peaks can be identified such as the two near  $1650\text{ cm}^{-1}$  (Amide I: C=O bond vibration, C-N and N-H bonds stretching) and  $1550\text{ cm}^{-1}$  ( Amide II: C-N and N-H bonds vibration) [55]. These bands can be largely attributed to the presence of milk proteins and peptides on the surface of the membranes [56].

The large peak around  $3300\text{ cm}^{-1}$  corresponding to N-H bond stretching in Amide A also relates to the presence of proteins [57,58]. The Peak located at  $1080\text{ cm}^{-1}$  can be attributed to lactose (C-O) and lactic acid [58,59]. The peaks absorbed at wavelengths around  $2900\text{ cm}^{-1}$  correspond to a strong aliphatic C-H stretch and could correspond to lactose, proteins, fatty acids but also nisin [56,57,60,61]. No peaks specifically attributed to lipid compounds were identified, which is consistent with the fact that skim milk was used as a medium for the production of nisin. Sodium citrate, which is normally present in the medium, also does not appear to be present.

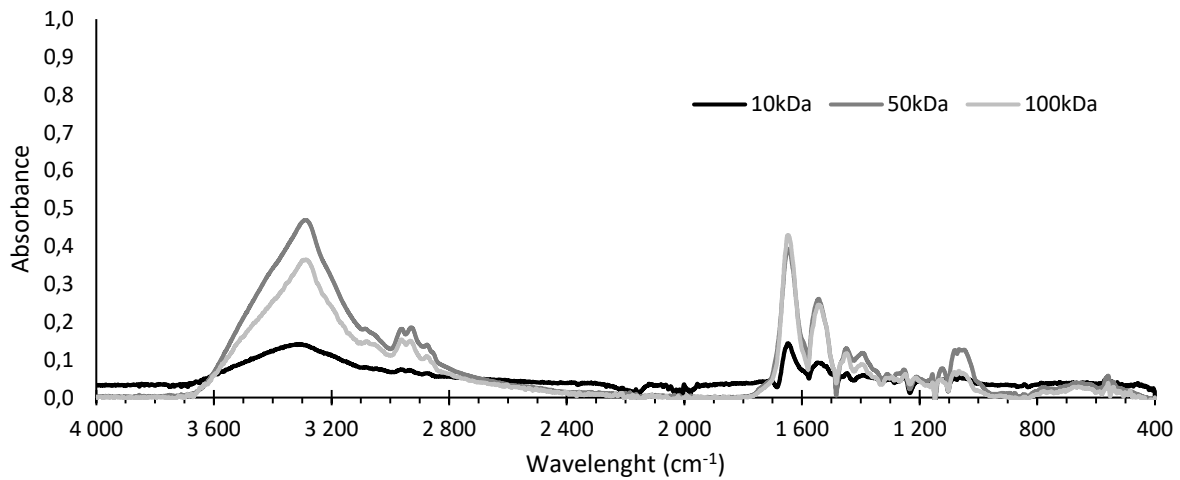


**Figure 7: ATR-FTIR spectra of foulants deposited on the membranes.**

Therefore, according to the results, it can be suggested that the membrane irreversible foulants consisted mainly of proteins. Comparing the signals between all membranes tested shows that 50 and 100 kDa were more affected by irreversible fouling than the 10 kDa membrane. This result is in contrast to Section 3.3.2 where it was shown that the 100 kDa membrane was the most prone to reversible fouling and that the  $R_{rev}/R_{fc}$  ratio was almost identical for 10 kDa and 50 kDa membranes.

### 3.3.4. Possible fouling mechanisms

Membrane fouling in biotechnology mainly arises from the composition and properties of the feed solution apart from the effects of operation parameters (pressure, temperature, flow rate...). As shown

in Table 4, the feed presents a complex multicomponent aqueous matrix containing macromolecules (milk proteins, peptides) and small molecules (amino acids, salts, sugars, etc.). All these components could be involved in the membrane fouling. According to their ability to permeate the membrane, one can distinguish a fouling inside the pore or at the supernatant/membrane interface or in the accumulated layer outside of the membrane.

In order to elucidate the fouling mechanisms of membranes during the ultrafiltration of supernatants, the data on permeate flux reduction (Figure 4) were fitted to Hermia's model linear equations (Table 2). Table 7 shows the values of  $R^2$  and the estimated constants for all of the linear equations.

**Table 7. Values of  $R^2$  and estimated constants of Hermia's model linear equations for membranes under study**

Model	Parameter	10 kDa	50 kDa	100 kDa
<b>n = 2</b>	$R^2$	0.9209	0.9880	0.9501
	$k_c \times 10^5$	3.0	7.0	7.0
<b>n = 1.5</b>	$R^2$	0.9484	0.9921	0.9460
	$K_p \times 10^6$	3.0	5.0	4.0
<b>n = 1</b>	$R^2$	0.9689	0.9940	0.9408
	$K_i \times 10^7$	10.0	10.0	7.0
<b>n = 0</b>	$R^2$	0.9911	0.9909	0.8996
	$K_t \times 10^9$	10.0	5.0	0.7

For the 10 kDa membrane, the cake formation model  $R^2$  value was higher than 0.98, suggesting that the predominant fouling mechanism for this membrane was cake formation and the next was intermediate pore blocking, while limited surface deposit ( $R^2 < 0.95$ ) occurred. In this situation, one can point out the physical phenomena that occur during ultrafiltration with this membrane. At the beginning of the ultrafiltration stage, intermediate pore blocking was the main fouling mechanism: a part of small amino acid molecules as well as sugars and peptides entered into the pores of the membrane, attached to wall, and thus led to internal membrane fouling. Then milk proteins, much larger than the membrane pore size, accumulated on the surface and formed a permeable cake layer. This analysis agrees with the results of resistance-in-series-model, in which reversible and irreversible resistances were relatively balanced.

In the case of 50 kDa membrane, the  $R^2$  values of the four linear models were higher than 0.98. In this case, it seems difficult to select the best appropriate model to describe the predominant fouling mechanism. According to other authors [62], the decrease in permeate flux during crossflow

ultrafiltration can be divided into several stages, taking into account different fouling mechanisms. This is probably the case with the 50 kDa membrane.

For the fouling of 100 kDa membrane, the most suitable model was the complete blocking model. This mechanism occurs when the size of the solute molecules in the feed solution is larger than the membrane pores. Therefore, solute molecules causing fouling do not enter the membrane pores and do not reach the permeate side. In the case of 100 kDa membrane, the prevalence of complete blocking mechanism can be associated to casein micelles which are considered to be the major foulants causing complete pore blocking in the UF of dairy feeds [63].

With respect to the values of the fitted Hermia's model parameters, the results of Table 8 show that the higher values of the Hermia's model constants were obtained with the 10 and 50 kDa membranes. This finding is consistent with the fouling index and flux decline results obtained with these membranes. In fact, the values of these parameters should be higher for the experimental conditions that correspond to a more severe fouling of the membranes which is expected based on the physical meaning and the definitions of the Hermia's model parameters [64,65].

### 3.4. Characterization of the membrane fractions

To characterize the fractions resulting from the ultrafiltration process, all retentates and permeates were analyzed with regard to protein content, protein size distribution, dry matter, ash, and antibacterial activity.

#### 3.4.1. Protein composition determination by SDS-PAGE

The protein composition of the various ultrafiltration fractions as well as initial supernatants and commercial nisin was examined by SDS-PAGE analyzes under reducing conditions (Fig. 8).

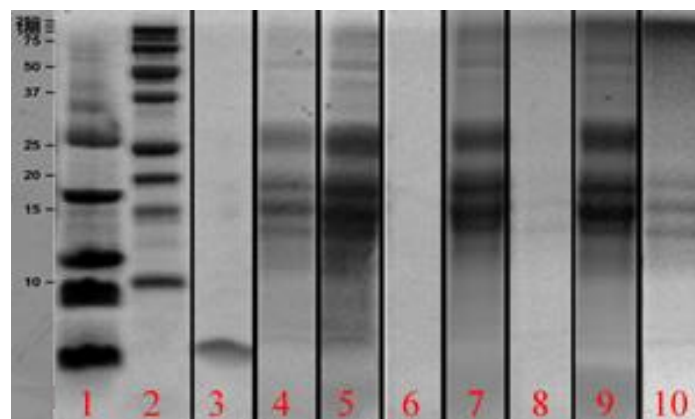


**Figure 8: Sodium dodecyl sulphate polyacrylamide gel electrophoresis (SDS-PAGE) profiles of supernatant, commercial nisin and ultrafiltration fractions with 10, 50 and 100 kDa MWCOs. Lanes: 1: molecular weight marker from 1.4 kDa to 26.6 kDa, 2: molecular weight markers ranging from 10 kDa to 250 kDa, 3: commercial nisin solution (250 mg. L<sup>-1</sup>), 4: supernatant, 5: 10 kDa retentate, 6: 10 kDa permeate, 7: 50 kDa retentate, 8: 50 kDa permeate, 9: 100 kDa retentate, 10: 100 kDa permeate.**

Although the commercially available nisin is a fermentation product, only one band with a molecular weight of 3.5 kDa is visible. This agrees with the molecular weight of nisin [6]. Different protein bands ranging from 3.5 to 250 kDa were obtained for initial supernatants (lane 4) and retentates (lanes 5, 7 and 9).

By analyzing the SDS-PAGE profile for fractions obtained with the 10 kDa membrane, it can be seen that no protein bands were detected in the permeate stream, including those corresponding to molecular weights less than 10 kDa. This result differs from what was observed from the total protein content measured in this fraction, in which 53.92% of proteins have permeated the membrane. This can be explained by the fact that proteins that passed through the 10 kDa membrane during the ultrafiltration are present as short peptides or as free amino acids, which are not visible as a band due to their low concentration or their presence in the migration front (not shown in the figure). In the retentate stream, it is evident that the protein bands were almost identical to the initial supernatant. The intensity of the protein bands in the retentate is higher than in the initial supernatant, especially for the 10-40 kDa range. In addition, proteins with a molecular weight of less than 10 kDa appear to be retained, even though this is the MWCO of the membrane. This finding suggests that the proteins form higher molecular weight structures. This applies in particular to nisin, which has the property of forming dimers (7,000 Da) and tetramers (14,000 Da) in solution [6]. It has also been reported in the literature that bacteriocins are retained very efficiently by UF membranes with a MWCO of 10 kDa [25]. Another explanation for the retention of proteins with a molecular weight lower than the MWCO of the membrane is the formation of a secondary cake layer as discussed in the previous section, which lowers the actual MWCO of the membrane and changes its separation/fractionation properties [63]. With a membrane fractionation at 50 kDa, considering the molecular weight of protein fractions identified in culture supernatants (14.2 to 66.4 kDa), it could be thought that proteins should pass through 50 kDa with ease. However, only four bands have appeared in the permeate. The one at ~3,35 kDa is only slightly visible and indicates that nisin could only partially pass through the membrane. The others bands are also only faintly visible and are between 15 and 25 kDa in term of size. This result could be attributed to protein aggregation processes which could be partly due to electrostatic environment effects, since the extent of aggregation of the proteins is pH-dependent. In fact, at culture supernatant pH 4.7, milk proteins are essentially uncharged according to their IEP, large aggregates of up to 8 molecules are formed through intermolecular interactions between protein monomers and result in low transmission of these proteins in permeate [66].

With the 100 kDa membrane, all bands below 50kDa are clearly visible in the permeate, even if their intensities are still lower than in the supernatant. Only the ~3.35 kDa band shows the same intensity as in the supernatant. On the retentate side there is also an intensification of all bands except the



~3.35 kDa band. From these results it can be seen that the selectivity of the membrane at 100kDa was also modified. On the other hand, nisin does not appear to be retained by the membrane at all.

#### **3.4.2. Dry matter, protein content and ash**

From ultrafiltration experiments, mass balances were performed to evaluate the dry matter, protein, and ash content of supernatant, permeate and retentate. Table 8 shows the process mass balance at VRF 5 for these components, where permeate (%) and retentate (%) are the component percentages (based on the supernatant content) in the permeate and retentate streams, respectively. This balance relates to the average of three experimental runs in which, starting from 500 mL of culture supernatant, 400 mL of the permeate and 50 mL of retentate were obtained. The dry matter, protein and ash content not contained in these streams is probably deposited in the membrane surface and in pores. This mass is presented in column  $m_{ret}$ .

**Table 8. Mass balance of the UF process referred to dry matter, protein and ash**

MWCO (kDa)		Permeate (%)	Retentate (%)	Balance (%)	$m_{ret}$ (g)
<b>10</b>	Dry matter	66.32	21.90	88.22	2.5657
	Protein	53.92	34.37	88.28	0.1374
	Ash	75.04	17.77	92.81	0.2428
<b>50</b>	Dry matter	72.05	22.07	94.12	1.1813
	Protein	53.94	37.19	91.14	0.0989
	Ash	76.73	19.20	95.93	0.1408
<b>100</b>	Dry matter	77.46	12.56	90.02	2.1749
	Protein	65.83	19.40	85.24	0.1723
	Ash	81.21	13.07	94.28	0.2058

From Table 8, it can be noted that the retention of investigated components was between 13.1 and 37.2 %. Low retention by the ultrafiltration process is expected since the culture supernatant contains small molecules such as salts, lactose, amino acids, organic acids and other small metabolites. These components could easily pass through the membrane pores into the permeate stream because their molecular mass was comparatively lower than the cut-off of the tested membranes. Similar retention behavior was observed between 10 and 50 kDa membranes. However, in the last two columns of Table 9, it is easy to see that the amounts of the deposited dry matter, protein and ash on the membrane were greatest for the 10 kDa membrane. It can also be observed that the 100 kDa membrane showed the lowest component retention.

With regard to protein, a relatively high protein content was observed in the permeates, which can be attributed to a high content of low-molecular protein compounds in the culture supernatants (peptides and aminoacids) compared to milk proteins. In addition, it was found that protein transmission for 10 and 50 kDa membranes was similar (53.92 and 53.94 %, respectively). However, the percentage of protein in the retentate was slightly lower for the 10 kDa membrane due to a higher protein deposition on the membrane. The similar behavior of 10 and 50 kDa membranes with respect to protein retention suggests that protein separation with these membranes is governed by the formation of milk protein agglomerates as discussed in the previous section, and the presence of a large proportion of low molecular weight protein molecules in the culture supernatants, capable of permeating these two membranes. The 100 kDa membrane showed the lowest percentage of protein in the retentate compared to 10 and 50 kDa membranes due to the size exclusion effect.

The selective capacity of each membrane relative to mineral components (ash) was also determined. The results presented in Table 9 showed that the retention of ash follows the same trend as for

proteins. The 10 and 50 kDa membranes showed similar retention results with a higher membrane deposition for the 10 kDa membrane. The 100 kDa membrane showed the lowest retention among the cut-offs tested.

### 3.5. Nisin activity, yield and purification factor

The potential separation efficiency on nisin using ultrafiltration was assessed. Supernatants and resulting permeates and retentates were tested for antimicrobial activity against the target strain *L. innocua*. The results are given in Table 9 and the purification factors obtained with membranes tested are shown graphically in Figure 7.

**Table 9. Purification parameters of the ultrafiltration with the tested membranes**

MWCO (kDa)	Fraction	Protein		Antimicrobial activity		
		Concentration (mg. mL <sup>-1</sup> )	Yield (%)	Activity (AU/mL)	Specific activity (AU/ mg protein)	Yield (%)
	Culture supernatant	2.84	100	64	22.54	100.0
10	Retentate	5.27	34.1	512	97.15	144.0
	Permeate	1.98	57.0	0	0.00	0.0
50	Retentate	4.49	34.7	256	57.02	65.6
	Permeate	1.50	58.0	16	10.67	20.5
100	Retentate	4.42	15.2	64	14.48	10.0
	Permeate	2.32	72.0	64	27.59	90.0

The antimicrobial activity obtained from the *L. lactis* DSM 20729 fermentation under our conditions was 64 UA. mL<sup>-1</sup>. In the case of the 10 and 50 kDa membranes, an increase in the antimicrobial activity in the retentate was observed. The results also show that 10 and 50 kDa membranes lead to a similar protein yield in the retentate and permeate fractions. All the antimicrobial activity was retained by the 10 kDa membrane during the ultrafiltration, with the antimicrobial activity in the retentate increasing 8-fold compared to the original supernatant. Permeates resulting from this MWCO had no antimicrobial activity. With a 50 kDa membrane, permeates had an antimicrobial effect, suggesting that nisin partially permeates the membrane. These results are compatible with those obtained with SDS-PAGE analysis. At 50 kDa MWCO, a 4-fold increase in activity and activity yield of 65.5% was achieved in the retentates. With a nisin size of 3.35 kDa, these data suggest that nisin occurs in high molecular weight aggregates which is consistent with the nisin property of forming dimers (7000 Da) and tetramers (14,000 Da) in solution. In addition, it is known that nisin undergoes electrostatic or

hydrophobic interactions with other proteins [67,68], which could explain the similar protein recovery and the nisin retention behavior for 10 and 50 kDa membranes. These nisin properties, associated with the modification of membrane selectivity during ultrafiltration, explain the full nisin retention with the 10kDa membrane and its partial retention with the 50 kDa membrane. For the 100 kDa membrane, the same activity per volume was measured in the permeate and in the retentate, which indicates a complete passage without retention with this MWCO, which agrees with the SDS-PAGE analysis. Muriana and Klaenhammer [69] reported similar observations wherein lactacin F (2.5 kDa) was completely recovered from the culture supernatant of *Lactobacillus acidophilus* by ultrafiltration in retentate from 100 and 300 kDa membranes. The authors explained this result by the association of lactacin with a larger molecular complex. They also stated that the formation of aggregates in solution can also be physically disrupted to yield additional units of activity. The activity balance (AB%) calculated for the membranes tested is shown in Table 10.

**Table 10. Antimicrobial activity balance (AB%) calculated for the tested membranes**

MWCO (kDa)	AB (%)
10	118.9 ± 33.0
50	70.0 ± 13.1
100	93.1 ± 9.8

We observed that the activity balance for the membranes tested was in the following order: 10 kDa>100 kDa>50 kDa. Mass balance calculations indicated that all the nisin originally present in the culture supernatant was recovered with the 10 kDa membrane. This was not the case with the 50kDa and 100kDa membranes, where a loss of activity was observed.

The purification factor ( $P_F$ ), as defined in Eq. (9), depends on the yield of nisin separation and the presence of impurities in the fractions. The purification factors are shown in Fig. 9 for the permeate and retentate fractions obtained with the three MWCOs tested.

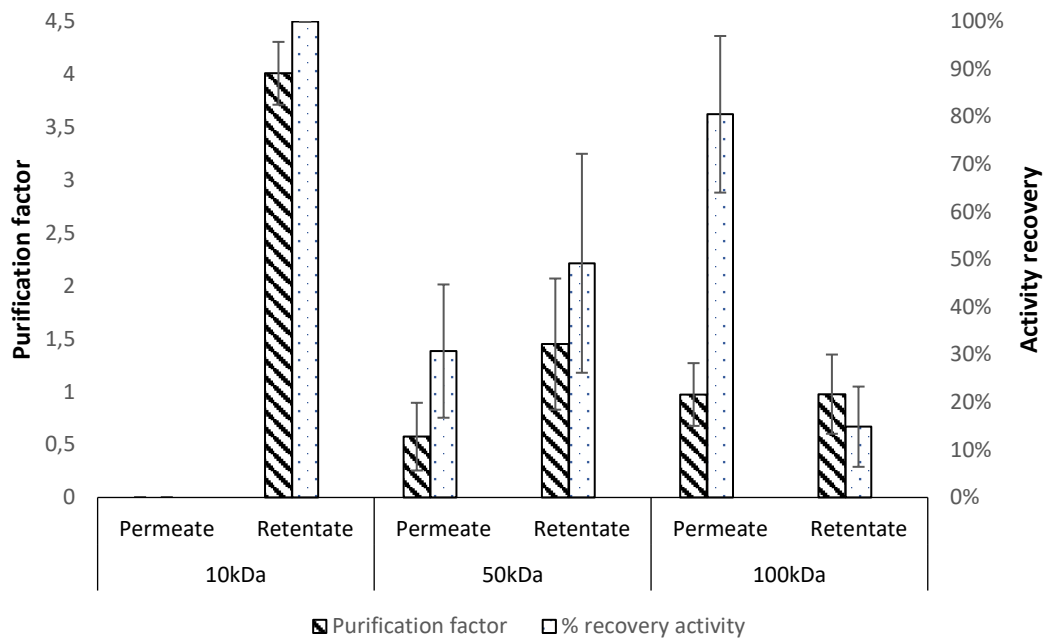


**Figure 9: Nisin recovery and purification factors in permeate and retentate streams with the tested membranes**

At 100 kDa, the purification factor in the permeate and in the retentate was about 1, which means that the nisin was not separated from the other proteins in the supernatant. This result is quite unexpected as it suggests that all proteins in the medium behaved like nisin with no membrane retention. Contrary to what the SDS PAGE results suggested, we were able to see a band intensification phenomenon in the retentate, usually reflecting an increase in protein concentration, and low intensity bands in the permeate with low intensity in the permeate which usually reflect a lower protein concentration. At 50kDa, the purification factor obtained for the retentate was about 1.5, which means that nisin was retained compared to other proteins. The highest purification factor was achieved in the retentate at 10kDa and reached a value of 4. This value could be increased by driving the ultrafiltration to a higher VRF.

In Table 11, we compare the purification parameters of conventional methods commonly used in the concentration stage during downstream processing of nisin and results obtained in this work.

**Table 11. Comparison of yield and fold purification values of nisin concentration processes**

<b>Separation method</b>	<b>Activity yield (%)</b>	<b>Purification factor</b>	<b>Reference</b>
<b>Ammonium sulfate precipitation</b>	98	5.07	[70]
	62	2.52	[71]
	94	3.80	[72]
	90	168.80	[14]
<b>Solvent extraction</b>			
<b>Chloroform</b>	70	23.40	[18]
	24	37.43	[14]
<b>Methanol</b>	91	5.3	[19]
<b>Ethanol</b>	85	5.5	[19]
<b>Ultrafiltration</b>	100	4.01	This work

It seems clear that the use of ultrafiltration in the case of nisin recovery may offer a viable option for large-scale production of this bacteriocin. The ultrafiltration methodology can also be refined by increasing the VRF and applying diafiltration. It is expected that further understanding of the interactions that occur between nisin and other compounds present in culture supernatants will lead to an improved design of the ultrafiltration process.

## **Conclusion**

In this work, ultrafiltration separation technology for the recovery and concentration of nisin from complex culture supernatants of *L. Lactis* was developed and demonstrated. To the best of our knowledge, no systematic study has been performed to investigate the effectiveness of ultrafiltration for the selective recovery of nisin contained in culture supernatants.

Three ultrafiltration membranes with different MWCO were screened. All membranes examined showed a decline of permeate flux - 94% for the 10 kDa membrane, 96% for the 50 kDa membrane, and 92% for the 100 kDa membrane. The resistance in series model and Hermia's model were applied to quantify the contribution of reversible and irreversible fouling of each membrane and investigate fouling mechanism during ultrafiltration. Reversible fouling was predominant in all three membranes studied. However, by fitting the experimental data to Hermia's model equations, the most suitable fouling mechanism was cake layer for 10 kDa membrane, intermediate pore blocking for 50 kDa membrane and complete blocking model for 100 kDa membrane. After water rinsing and chemical cleaning, a good recovery of the permeate flux was achieved with the exception of the 50 kDa membrane.

The 10-kDa membrane enabled the upmost recovery of nisin and the highest purification factor, achieving 100% and 4 in the retentate stream, respectively. The 50 kDa membrane, in turn, led to a lower antimicrobial activity yield and a lower purification factor of 65% and 1.5, respectively. Of note, the 100 kDa membrane showed no selectivity towards nisin. The results also showed that interactions between nisin and proteins contained in the culture supernatants can occur, which adversely can affect the nisin separation performance. It is expected that further understanding of the interactions that occur between nisin and other compounds present in culture supernatants will lead to an improved design of the ultrafiltration process.

Compared with other conventional separation and concentration methods in nisin downstream processing, ultrafiltration process has many advantages, such as simple equipment, convenient operation, and low energy consumption. In addition, it does not require organic solvents and the simplicity of the approach facilitates scale-up. Although fouling phenomena are important, these problems can be minimized by applying optimal operating conditions on a larger scale. The 10 kDa membrane seems to be the optimal membrane to use in further experiments that should focus on increasing the VRF and applying diafiltration to increase the purity of nisin in the retentate.

## **Funding**

The Financial support for this study was provided by the CPER-FEDER Alibiotech program funding (2016 – 2021) managed by the Hauts-de-France region.

## References

- [1] A. Besse, J. Peduzzi, S. Rebuffat, A. Carré-Mlouka, Antimicrobial peptides and proteins in the face of extremes: Lessons from archaeococci, *Biochimie*. 118 (2015) 344–355. <https://doi.org/10.1016/j.biochi.2015.06.004>.
- [2] T. Sidooski, A. Brandelli, S.L. Bertoli, C.K.D. Souza, L.F.D. Carvalho, Physical and nutritional conditions for optimized production of bacteriocins by lactic acid bacteria—A review, *Critical Reviews in Food Science and Nutrition*. 59 (2019) 2839–2849. <https://doi.org/10.1080/10408398.2018.1474852>.
- [3] S. Duquesne, D. Destoumieux-Garzón, J. Peduzzi, S. Rebuffat, Microcins, gene-encoded antibacterial peptides from enterobacteria, *Nat. Prod. Rep.* 24 (2007) 708–734. <https://doi.org/10.1039/B516237H>.
- [4] P. Alvarez-Sieiro, M. Montalbán-López, D. Mu, O.P. Kuipers, Bacteriocins of lactic acid bacteria: extending the family, *Applied Microbiology and Biotechnology*. 100 (2016) 2939–2951. <https://doi.org/10.1007/s00253-016-7343-9>.
- [5] L.J. de Arauz, A.F. Jozala, P.G. Mazzola, T.C.V. Penna, Nisin biotechnological production and application: a review, *Trends in Food Science & Technology*. 20 (2009) 146–154. <https://doi.org/10.1016/j.tifs.2009.01.056>.
- [6] A. Gharsallaoui, N. Oulahal, C. Joly, P. Degraeve, Nisin as a Food Preservative: Part 1: Physicochemical Properties, Antimicrobial Activity, and Main Uses, *Null*. 56 (2016) 1262–1274. <https://doi.org/10.1080/10408398.2013.763765>.
- [7] S. Khelissa, N.-E. Chihib, A. Gharsallaoui, Conditions of nisin production by *Lactococcus lactis* subsp. *lactis* and its main uses as a food preservative, *Archives of Microbiology*. 203 (2021) 465–480. <https://doi.org/10.1007/s00203-020-02054-z>.
- [8] P.D. Cotter, C. Hill, R.P. Ross, Bacteriocins: developing innate immunity for food, *Nature Reviews Microbiology*. 3 (2005) 777–788. <https://doi.org/10.1038/nrmicro1273>.
- [9] J.M. Shin, J.W. Gwak, P. Kamarajan, J.C. Fenno, A.H. Rickard, Y.L. Kapila, Biomedical applications of nisin, *Journal of Applied Microbiology*. 120 (2016) 1449–1465. <https://doi.org/10.1111/jam.13033>.
- [10] Z.J. Ng, M.A. Zarin, C.K. Lee, J.S. Tan, Application of bacteriocins in food preservation and infectious disease treatment for humans and livestock: a review, *RSC Adv.* 10 (2020) 38937–38964. <https://doi.org/10.1039/D0RA06161A>.
- [11] W. Liu, Improvement of nisin production by using the integration strategy of co-cultivation fermentation, foam fractionation and pervaporation, (2021) 9.
- [12] S. Oshima, A. Hirano, H. Kamikado, J. Nishimura, Y. Kawai, T. Saito, Nisin A extends the shelf life of high-fat chilled dairy dessert, a milk-based pudding, *Journal of Applied Microbiology*. 116 (2014) 1218–1228. <https://doi.org/10.1111/jam.12454>.
- [13] European Food Safety Authority (EFSA), Opinion of the Scientific Panel on food additives, flavourings, processing aids and materials in contact with food (AFC) related to the safety in use of nisin as a food additive in an additional category of liquid eggs, *EFSA Journal*. 4 (2006) 314b. <https://doi.org/10.2903/j.efsa.2006.314b>.
- [14] S.H. Tafreshi, S. Mirdamadi, S. Khatami, Comparison of Different Nisin Separation and Concentration Methods: Industrial and Cost-Effective Perspectives, *Probiotics & Antimicro. Prot.* 12 (2020) 1226–1234. <https://doi.org/10.1007/s12602-019-09607-9>.
- [15] V. Kaškonienė, M. Stankevičius, K. Bimbraitė-Survilienė, G. Naujokaitytė, L. Šernienė, K. Mulkytė, M. Malakauskas, A. Maruška, Current state of purification, isolation and analysis of bacteriocins produced by lactic acid bacteria, *Applied Microbiology and Biotechnology*. 101 (2017) 1323–1335. <https://doi.org/10.1007/s00253-017-8088-9>.
- [16] E. Twomey, C. Hill, D. Field, M. Begley, Recipe for Success: Suggestions and Recommendations for the Isolation and Characterisation of Bacteriocins, *Int J Microbiol.* 2021 (2021) 9990635–9990635. <https://doi.org/10.1155/2021/9990635>.



- [17] N.A. Kelly, B.G. Reuben, J. Rhoades, S. Roller, Solvent extraction of bacteriocins from model solutions and fermentation broths, *Journal of Chemical Technology & Biotechnology*. 75 (2000) 777–784. [https://doi.org/10.1002/1097-4660\(200009\)75:9<777::AID-JCTB290>3.0.CO;2-0](https://doi.org/10.1002/1097-4660(200009)75:9<777::AID-JCTB290>3.0.CO;2-0).
- [18] L.L. Burianek, A.E. Yousef, Solvent extraction of bacteriocins from liquid cultures, *Letters in Applied Microbiology*. 31 (2000) 193–197. <https://doi.org/10.1046/j.1365-2672.2000.00802.x>.
- [19] D. Xiao, P.M. Davidson, D.H. D'Souza, J. Lin, Q. Zhong, Nisin extraction capacity of aqueous ethanol and methanol from a 2.5% preparation, *Journal of Food Engineering*. 100 (2010) 194–200. <https://doi.org/10.1016/j.jfoodeng.2010.03.044>.
- [20] A.F. Jozala, A.M. Lopes, P.G. Mazzola, P.O. Magalhães, T.C.V. Penna, A. Pessoa, Liquid–liquid extraction of commercial and biosynthesized nisin by aqueous two-phase micellar systems, *Enzyme and Microbial Technology*. 42 (2008) 107–112. <https://doi.org/10.1016/j.enzmictec.2007.08.005>.
- [21] A.F. Jozala, A.M. Lopes, L.C. de Lencastre Novaes, P.G. Mazzola, T.C.V. Penna, A.P. Junior, Aqueous Two-phase micellar system for nisin extraction in the presence of electrolytes, *Food Bioprocess Technol*. 6 (2013) 3456.
- [22] R. Castro-Muñoz, G. Boczkaj, E. Gontarek, A. Cassano, V. Fila, Membrane technologies assisting plant-based and agro-food by-products processing: A comprehensive review, *Trends in Food Science & Technology*. 95 (2020) 219–232. <https://doi.org/10.1016/j.tifs.2019.12.003>.
- [23] M.-P. Zacharof, G.M. Coss, S.J. Mandale, R.W. Lovitt, Separation of lactobacilli bacteriocins from fermented broths using membranes, *Process Biochemistry*. 48 (2013) 1252–1261. <https://doi.org/10.1016/j.procbio.2013.05.017>.
- [24] J. Zhang, Y. Zhang, Y. Wen, Q. Gao, D. Wang, M. Zhao, Y. Han, Z. Zhou, A Compatible Membrane Process for Separation and Concentration of Pediocin PA-1 from Fermentation Broth, *Separation Science and Technology (Philadelphia)*. 49 (2014) 1978–1984. <https://doi.org/10.1080/01496395.2014.905598>.
- [25] S. Ohmomo, S. Murata, N. Katayama, S. Nitisinprasart, M. Kobayashi, T. Nakajima, M. Yajima, K. Nakanishi, Purification and some characteristics of enterocin ON-157, a bacteriocin produced by *Enterococcus faecium* NIAI 157, *Journal of Applied Microbiology*. 88 (2000) 81–89. <https://doi.org/10.1046/j.1365-2672.2000.00866.x>.
- [26] H. Daba, S. Pandian, J.F. Gosselin, R.E. Simard, J. Huang, C. Lacroix, Detection and activity of a bacteriocin produced by *Leuconostoc mesenteroides*, *Appl. Environ. Microbiol*. 57 (1991) 3450–3455.
- [27] M. Doria, A. Ferrara, A. Auricchio, AAV2/8 Vectors Purified from Culture Medium with a Simple and Rapid Protocol Transduce Murine Liver, Muscle, and Retina Efficiently, *Human Gene Therapy Methods*. 24 (2013) 392–398. <https://doi.org/10.1089/hgtb.2013.155>.
- [28] C. Conidi, A. Cassano, F. Caiazzo, E. Drioli, Separation and purification of phenolic compounds from pomegranate juice by ultrafiltration and nanofiltration membranes, *Journal of Food Engineering*. 195 (2017) 1–13. <https://doi.org/10.1016/j.jfoodeng.2016.09.017>.
- [29] E.M. Romero-Dondiz, J.E. Almazán, V.B. Rajal, E.F. Castro-Vidaurre, Removal of vegetable tannins to recover water in the leather industry by ultrafiltration polymeric membranes, *Chemical Engineering Research and Design*. 93 (2015) 727–735. <https://doi.org/10.1016/j.cherd.2014.06.022>.
- [30] J. HERMIA, CONSTANT PRESSURE BLOCKING FILTRATION LAWS - APPLICATION TO POWER-LAW NON-NEWTONIAN FLUIDS., *TRANS INST CHEM ENG*. V 60 (1982) 183–187.

- [31] R. Gough, B. Gómez-Sala, P.M. O'Connor, M.C. Rea, S. Miao, C. Hill, A. Brodkorb, A Simple Method for the Purification of Nisin, *Probiotics & Antimicro. Prot.* 9 (2017) 363–369. <https://doi.org/10.1007/s12602-017-9287-5>.
- [32] M. Costas Malvido, E. Alonso González, N. Pérez Guerra, Nisin production in realkalized fed-batch cultures in whey with feeding with lactose- or glucose-containing substrates, *Appl Microbiol Biotechnol.* 100 (2016) 7899–7908. <https://doi.org/10.1007/s00253-016-7558-9>.
- [33] S. Jovanovic, M. Barac, O. Macej, T. Vucic, C. Lacnjevac, SDS-PAGE Analysis of Soluble Proteins in Reconstituted Milk Exposed to Different Heat Treatments, *Sensors (Basel).* 7 (2007) 371–383.
- [34] A. Mookoolall, L. Sykora, J. Pfanstiel, S. Nöbel, J. Weiss, J. Hinrichs, A feasibility study on the application of a laccase-mediator system in stirred yoghurt at the pilot scale, *Food Hydrocolloids.* 60 (2016) 119–127. <https://doi.org/10.1016/j.foodhyd.2016.03.027>.
- [35] P.D. Veith, E.C. Reynolds, Production of a High Gel Strength Whey Protein Concentrate from Cheese Whey, *Journal of Dairy Science.* 87 (2004) 831–840. [https://doi.org/10.3168/jds.S0022-0302\(04\)73227-0](https://doi.org/10.3168/jds.S0022-0302(04)73227-0).
- [36] N.S. Krishna Kumar, M.K. Yea, M. Cheryan, Ultrafiltration of soy protein concentrate: performance and modelling of spiral and tubular polymeric modules, *Journal of Membrane Science.* 244 (2004) 235–242. <https://doi.org/10.1016/j.memsci.2004.06.056>.
- [37] W. Doyen, W. Adriansens, B. Molenberghs, R. Leysen, A comparison between polysulfone, zirconia and organo-mineral membranes for use in ultrafiltration, *Journal of Membrane Science.* 113 (1996) 247–258. [https://doi.org/10.1016/0376-7388\(95\)00124-7](https://doi.org/10.1016/0376-7388(95)00124-7).
- [38] S.R. Wickramasinghe, B. Kalbfuß, A. Zimmermann, V. Thom, U. Reichl, Tangential flow microfiltration and ultrafiltration for human influenza A virus concentration and purification, *Biotechnology and Bioengineering.* 92 (2005) 199–208. <https://doi.org/10.1002/bit.20599>.
- [39] Y. Sun, Z. Qin, L. Zhao, Q. Chen, Q. Hou, H. Lin, L. Jiang, J. Liu, Z. Du, Membrane fouling mechanisms and permeate flux decline model in soy sauce microfiltration, *Journal of Food Process Engineering.* 41 (2018) e12599. <https://doi.org/10.1111/jfpe.12599>.
- [40] C. Baldasso, T.C. Barros, I.C. Tessaro, Concentration and purification of whey proteins by ultrafiltration, *Desalination.* 278 (2011) 381–386. <https://doi.org/10.1016/j.desal.2011.05.055>.
- [41] R. Atrá, G. Vatai, E. Bekassy-Molnar, A. Balint, Investigation of ultra- and nanofiltration for utilization of whey protein and lactose, *Journal of Food Engineering.* 67 (2005) 325–332. <https://doi.org/10.1016/j.jfoodeng.2004.04.035>.
- [42] P. Bacchin, P. Aimar, R.W. Field, Critical and sustainable fluxes: Theory, experiments and applications, *Journal of Membrane Science.* 281 (2006) 42–69. <https://doi.org/10.1016/j.memsci.2006.04.014>.
- [43] Z. Yang, Y.-C. Juang, D.-J. Lee, Y.-Y. Duan, Pore blockage of organic fouling layer with highly heterogeneous structure in membrane filtration: Role of minor organic foulants, *Journal of Membrane Science.* 411–412 (2012) 30–34. <https://doi.org/10.1016/j.memsci.2012.04.010>.
- [44] M. Szczygielka, K. Prochaska, Downstream separation and purification of bio-based alpha-ketoglutaric acid from post-fermentation broth using a multi-stage membrane process, *Process Biochemistry.* 96 (2020) 38–48. <https://doi.org/10.1016/j.procbio.2020.05.026>.
- [45] H.-L. Chen, Y.-S. Chen, R.-S. Juang, Recovery of surfactin from fermentation broths by a hybrid salting-out and membrane filtration process, *Separation and Purification Technology.* 59 (2008) 244–252. <https://doi.org/10.1016/j.seppur.2007.06.010>.

- [46] S. Mondal, C. Rai, S. De, Identification of Fouling Mechanism During Ultrafiltration of Stevia Extract, *Food and Bioprocess Technology*. 6 (2013) 931–940. <https://doi.org/10.1007/s11947-011-0754-9>.
- [47] A. Aouni, C. Fersi, B. Cuartas-Uribe, A. Bes-Piá, M.I. Alcaina-Miranda, M. Dhahbi, Study of membrane fouling using synthetic model solutions in UF and NF processes, *Chemical Engineering Journal*. 175 (2011) 192–200. <https://doi.org/10.1016/j.cej.2011.09.093>.
- [48] S.F.E. Boerlage, M.D. Kennedy, M.R. Dickson, D.E.Y. El-Hodali, J.C. Schippers, The modified fouling index using ultrafiltration membranes (MFI-UF): characterisation, filtration mechanisms and proposed reference membrane, *Journal of Membrane Science*. 197 (2002) 1–21. [https://doi.org/10.1016/S0376-7388\(01\)00618-4](https://doi.org/10.1016/S0376-7388(01)00618-4).
- [49] X. Zhao, R. Zhang, Y. Liu, M. He, Y. Su, C. Gao, Z. Jiang, Antifouling membrane surface construction: Chemistry plays a critical role, *Journal of Membrane Science*. 551 (2018) 145–171. <https://doi.org/10.1016/j.memsci.2018.01.039>.
- [50] J. Garcia-Ivars, M.-I. Alcaina-Miranda, M.-I. Iborra-Clar, J.-A. Mendoza-Roca, L. Pastor-Alcañiz, Enhancement in hydrophilicity of different polymer phase-inversion ultrafiltration membranes by introducing PEG/Al<sub>2</sub>O<sub>3</sub> nanoparticles, *Separation and Purification Technology*. 128 (2014) 45–57. <https://doi.org/10.1016/j.seppur.2014.03.012>.
- [51] A. Rahimpour, S.S. Madaeni, Improvement of performance and surface properties of nano-porous polyethersulfone (PES) membrane using hydrophilic monomers as additives in the casting solution, *Journal of Membrane Science*. 360 (2010) 371–379. <https://doi.org/10.1016/j.memsci.2010.05.036>.
- [52] F. Qu, H. Liang, J. Zhou, J. Nan, S. Shao, J. Zhang, G. Li, Ultrafiltration membrane fouling caused by extracellular organic matter (EOM) from *Microcystis aeruginosa*: Effects of membrane pore size and surface hydrophobicity, *Journal of Membrane Science*. 449 (2014) 58–66. <https://doi.org/10.1016/j.memsci.2013.07.070>.
- [53] T.-H. Bae, T.-M. Tak, Interpretation of fouling characteristics of ultrafiltration membranes during the filtration of membrane bioreactor mixed liquor, *Journal of Membrane Science*. 264 (2005) 151–160. <https://doi.org/10.1016/j.memsci.2005.04.037>.
- [54] P.D. Peeva, A.E. Palupi, M. Ulbricht, Ultrafiltration of humic acid solutions through unmodified and surface functionalized low-fouling polyethersulfone membranes – Effects of feed properties, molecular weight cut-off and membrane chemistry on fouling behavior and cleanability, *Separation and Purification Technology*. 81 (2011) 124–133. <https://doi.org/10.1016/j.seppur.2011.07.005>.
- [55] M.J. Luján-Facundo, J.A. Mendoza-Roca, B. Cuartas-Uribe, S. Álvarez-Blanco, Evaluation of cleaning efficiency of ultrafiltration membranes fouled by BSA using FTIR–ATR as a tool, *Journal of Food Engineering*. 163 (2015) 1–8. <https://doi.org/10.1016/j.jfoodeng.2015.04.015>.
- [56] J. Andrade, C.G. Pereira, J.C. de A. Junior, C.C.R. Viana, L.N. de O. Neves, P.H.F. da Silva, M.J.V. Bell, V. de C. dos Anjos, FTIR-ATR determination of protein content to evaluate whey protein concentrate adulteration, *LWT*. 99 (2019) 166–172. <https://doi.org/10.1016/j.lwt.2018.09.079>.
- [57] M. Aslam, F. Wicaksana, M. Farid, A. Wong, W.B. Krantz, Mitigation of membrane fouling by whey protein via water hammer, *Journal of Membrane Science*. 642 (2022) 119967. <https://doi.org/10.1016/j.memsci.2021.119967>.
- [58] I. Elsohaby, J.T. McClure, C.B. Riley, J. Bryanton, K. Bigsby, R.A. Shaw, Transmission infrared spectroscopy for rapid quantification of fat, protein, and lactose concentrations in human milk, *Journal of Perinatology*. 38 (2018) 1685–1693. <https://doi.org/10.1038/s41372-018-0233-5>.

- [59] M. Rabiller-Baudry, M.L. Maux, B. Chaufer, L. Begoin, Characterisation of cleaned and fouled membrane by ATR—FTIR and EDX analysis coupled with SEM: application to UF of skimmed milk with a PES membrane, *Desalination*. 146 (2002) 123–128. [https://doi.org/10.1016/S0011-9164\(02\)00503-9](https://doi.org/10.1016/S0011-9164(02)00503-9).
- [60] S. Belfer, R. Fainchtain, Y. Purinson, O. Kedem, Surface characterization by FTIR-ATR spectroscopy of polyethersulfone membranes-unmodified, modified and protein fouled, *Journal of Membrane Science*. 172 (2000) 113–124. [https://doi.org/10.1016/S0376-7388\(00\)00316-1](https://doi.org/10.1016/S0376-7388(00)00316-1).
- [61] S. Sadiq, M. Imran, H. Habib, S. Shabbir, A. Ihsan, Y. Zafar, F.Y. Hafeez, Potential of monolaurin based food-grade nano-micelles loaded with nisin Z for synergistic antimicrobial action against *Staphylococcus aureus*, *LWT - Food Science and Technology*. 71 (2016) 227–233. <https://doi.org/10.1016/j.lwt.2016.03.045>.
- [62] M.-J. Corbatón-Báguena, S. Álvarez-Blanco, M.-C. Vincent-Vela, Fouling mechanisms of ultrafiltration membranes fouled with whey model solutions, *Desalination*. 360 (2015) 87–96. <https://doi.org/10.1016/j.desal.2015.01.019>.
- [63] K.S.Y. Ng, M. Haribabu, D.J.E. Harvie, D.E. Dunstan, G.J.O. Martin, Mechanisms of flux decline in skim milk ultrafiltration: A review, *Journal of Membrane Science*. 523 (2017) 144–162. <https://doi.org/10.1016/j.memsci.2016.09.036>.
- [64] A.S. Cassini, I.C. Tessaro, L.D.F. Marczak, Ultrafiltration of wastewater from isolated soy protein production: Fouling tendencies and mechanisms, *Separation Science and Technology*. 46 (2011) 1077–1086. <https://doi.org/10.1080/01496395.2010.551045>.
- [65] M.C.V. Vela, S.Á. Blanco, J.L. García, E.B. Rodríguez, Analysis of membrane pore blocking models applied to the ultrafiltration of PEG, *Separation and Purification Technology*. 62 (2008) 489–498. <https://doi.org/10.1016/j.seppur.2008.02.028>.
- [66] M.C. Almécija, R. Ibáñez, A. Guadix, E.M. Guadix, Effect of pH on the fractionation of whey proteins with a ceramic ultrafiltration membrane, *Journal of Membrane Science*. 288 (2007) 28–35. <https://doi.org/10.1016/j.memsci.2006.10.021>.
- [67] V.N. Scott, S.L. Taylor, Effect of Nisin on the Outgrowth of *Clostridium botulinum* Spores, *J Food Science*. 46 (1981) 117–126. <https://doi.org/10.1111/j.1365-2621.1981.tb14543.x>.
- [68] J. Cleveland, M. Chikindas, T.J. Montville, Multimethod assessment of commercial nisin preparations, *Journal of Industrial Microbiology and Biotechnology*. 29 (2002) 228–232. <https://doi.org/10.1038/sj.jim.7000315>.
- [69] P.M. Muriana, T.R. Klaenhammer, Purification and partial characterization of lactacin F, a bacteriocin produced by *Lactobacillus acidophilus* 11088, *Applied and Environmental Microbiology*. 57 (1991) 114–121. <https://doi.org/10.1128/aem.57.1.114-121.1991>.
- [70] H.-J. Choi, C.-I. Cheigh, S.-B. Kim, Y.-R. Pyun, Production of a nisin-like bacteriocin by *Lactococcus lactis* subsp. *lactis* A164 isolated from Kimchi, *Journal of Applied Microbiology*. 88 (2000) 563–571. <https://doi.org/10.1046/j.1365-2672.2000.00976.x>.
- [71] S.S. Gujarathi, S.B. Bankar, L.A. Ananthanarayan, Fermentative Production, Purification and Characterization of Nisin, *International Journal of Food Engineering*. 4 (2008). <https://doi.org/10.2202/1556-3758.1386>.
- [72] K.-H. Lee, G.-S. Moon, J.-Y. An, H.-J. Lee, H.-C. Chang, D.K. Chung, J.-H. Lee, J.H. Kim, Isolation of a nisin-producing *Lactococcus lactis* strain from Kimchi and characterization of its *nisZ* gene, *Journal of Microbiology and Biotechnology*. 12 (2002) 389–397.